



HAL
open science

Mandibular-pelvic-patellar syndrome (mpp) is a novel pitx1-related disorder due to alteration of pitx1 transactivation ability

Godelieve Morel, Celine Duhamel, Simon BouSSION, Frederic Frenois, Gaetan Lesca, Nicolas Chatron, Audrey Labalme, Damien Sanlaville, Patrick Edery, Julien Thevenon, et al.

► To cite this version:

Godelieve Morel, Celine Duhamel, Simon BouSSION, Frederic Frenois, Gaetan Lesca, et al.. Mandibular-pelvic-patellar syndrome (mpp) is a novel pitx1-related disorder due to alteration of pitx1 transactivation ability. Human Mutation, 2020, Human mutation, 41 (9), pp.1499-1506. 10.1002/humu.24070 . hal-03405413

HAL Id: hal-03405413

<https://hal.univ-lille.fr/hal-03405413v1>

Submitted on 21 Feb 2025

HAL is a multi-disciplinary open access archive for the deposit and dissemination of scientific research documents, whether they are published or not. The documents may come from teaching and research institutions in France or abroad, or from public or private research centers.




L'archive ouverte pluridisciplinaire **HAL**, est destinée au dépôt et à la diffusion de documents scientifiques de niveau recherche, publiés ou non, émanant des établissements d'enseignement et de recherche français ou étrangers, des laboratoires publics ou privés.



Distributed under a Creative Commons Attribution 4.0 International License

BRIEF REPORT

Mandibular-pelvic-patellar syndrome is a novel *PITX1*-related disorder due to alteration of *PITX1* transactivation ability

Godelieve Morel^{1,2} | Céline Duhamel³ | Simon BouSSION³ | Frédéric Frénois³ | Gaetan Lesca^{2,4} | Nicolas Chatron^{2,4}  | Audrey Labalme² | Damien Sanlaville^{2,4} | Patrick Edery^{2,4} | Julien Thevenon⁵ | Laurence Faivre⁶ | Alice Fassier⁷ | Olivier Prodhomme⁸ | Fabienne Escande^{3,9} | Sylvie Manouvrier^{3,10} | Florence Petit^{3,10}  | David Geneviève¹¹ | Massimiliano Rossi^{2,4} 

¹Service de Génétique, Centre de compétences Anomalies du Développement, CHU de Nice, Nice, France

²Service de Génétique, Centre de Référence Anomalies du Développement et Centre de Compétences Maladies Osseuses Constitutionnelles, Hospices Civils de Lyon, Bron, France

³Université de Lille, Lille, France

⁴INSERM U1028, CNRS UMR5292, Centre de Recherche en Neurosciences de Lyon, GENDEV Team, Bron, France

⁵Service de Génétique, CHU de Grenoble, site Nord, France

⁶Service de Génétique, Centre de Référence Anomalies du Développement, FHU TRANSLAD, Hôpital d'Enfants, CHU de Dijon, and Inserm - Université de Bourgogne UMR1231 GAD, FHU-TRANSLAD, Dijon, France

⁷Service d'orthopédie pédiatrique, Centre de Compétences Maladies Osseuses Constitutionnelles, Hospices Civils de Lyon, Bron, France

⁸Service d'imagerie pédiatrique, Hôpital Arnaud de Villeneuve, CHU Montpellier, France

⁹Institut de Biochimie et Génétique moléculaire, CBP, CHU de Lille, France

¹⁰CHU Lille, Clinique de Génétique, Hôpital Jeanne de Flandre, Lille, France

¹¹Département de Génétique, IRMB, Maladies Rares et Médecine Personnalisée, Centre de Référence Maladies Rares ADSOOR, Filière AnDDI-Rare, INSERM U1183, CHU Montpellier, Université Montpellier, Montpellier, France

Correspondence

Massimiliano Rossi, Service de Génétique, Centre de Référence des Anomalies du Développement et Centre de Compétences Maladies Osseuses Constitutionnelles, Hospices Civils de Lyon, 59 boulevard Pinel, 69677 Bron Cedex, France.
Email: massimiliano.rossi01@chu-lyon.fr

Abstract

PITX1 is a homeobox transcription factor essential for hindlimb morphogenesis. Two *PITX1*-related human disorders have been reported to date: *PITX1* ectopic expression causes Liebenberg syndrome, characterized by malformation of upper limbs showing a “lower limb” appearance; *PITX1* deletions or missense variation cause a syndromic picture including clubfoot, tibial hemimelia, and preaxial polydactyly. We report two novel *PITX1* missense variants, altering *PITX1* transactivation ability, in three individuals from two unrelated families showing a distinct recognizable autosomal dominant syndrome, including first branchial arch, pelvic, patellar, and male genital abnormalities. This syndrome shows striking similarities with the *Pitx1*^{-/-} mouse model. A partial phenotypic overlap is also observed with Ischiocoxopodopatellar syndrome caused by *TBX4* haploinsufficiency, and with the phenotypic spectrum caused by *SOX9* anomalies, both genes being *PITX1* downstream targets. Our study findings expand the spectrum of *PITX1*-related disorders and

David Geneviève and Massimiliano Rossi contributed equally to this study.

suggest a common pattern of developmental abnormalities in disorders of the *PITX1-TBX4-SOX9* signaling pathway.

KEYWORDS

cleft palate, genital, patella, pelvis, Pierre-Robin, *PITX1*

The paired-like homeodomain transcription factor 1 gene (*PITX1*; MIM# 602149) encodes a bicoid homeobox containing transcription factor essential for hindlimb morphogenesis (Duboc & Logan, 2011). *PITX1* is mostly expressed in the lateral mesenchyme and developing hindlimb bud, the pituitary gland and the derivatives of the first branchial arch. Two *PITX1*-related human disorders (*PITX1*-RD) have been reported to date. Liebenberg syndrome (MIM# 186550), due to *PITX1* ectopic expression, is characterized by malformed upper limbs showing a “lower limb appearance” (Al-Qattan, Al-Thunayan, Alabdulkareem, & Al Balwi, 2013; Liebenberg, 1973). *PITX1* deletions or the missense variant p.(Glu130Lys) cause a syndromic picture (MIM# 119800) including clubfoot, tibial hemimelia, and preaxial polydactyly (Alvarado et al., 2011; Gurnett et al., 2008; Klopocki et al., 2012; Rosenfeld et al., 2011).

We report two novel *PITX1* missense variants, altering *PITX1* transactivation ability, in three individuals from two unrelated families showing a distinct recognizable syndrome, which, to the best of our knowledge, has not been previously described.

The three individuals were evaluated by clinical geneticists in two French Referral Centers for developmental abnormalities (Lyon and Montpellier). Genetic tests were performed as part of the routine etiological assessment, according to French laws and local ethic committees. Specific written informed consent for publication was obtained from the two families.

Concerning molecular analyses, for Individuals 1 and 2, exome capture was performed using SureSelect Clinical Research Exome Kit (Agilent). The resulting libraries were paired-end sequenced (2 × 150 bp) on a NextSeq 500 (Illumina). For Individual 3, exome capture was performed using Agilent in-solution enrichment methodology (SureSelect Human All Exon Kits Version 5, Agilent) with their biotinylated oligonucleotides probes library (Human All Exon v5–50 Mb, Agilent), followed by paired-end 75 bases massively parallel sequencing on Illumina HiSeq 2500.

Three-dimensional (3D) protein modeling prediction of the human missense variant of DNA-binding domain (DBD) of *PITX1* protein was carried out with the Phyre2 server (Protein Homology/analogy Recognition Engine V2.0). We compared the deduced human amino-acid 3D structure with the 3D resolved structure of the *Homo sapiens* DBD of *PITX2* protein (95% sequence identity) using the PyMOL Molecular Graphics System (v2.0, Schrödinger, LLC). The SuperPose server v.1.0 (Maiti, Van Domselaar, Zhang, & Wishart, 2004) was used to estimate the structural homology, measuring the average distance between the backbones of superimposed proteins.

The pCMV6-XL5-*PITX1* and TK-Bic-Luc plasmids were kindly provided by Christina A. Gurnett (Washington University). *PITX1*

variants c.412A>C and c.793G>T were introduced by site-directed mutagenesis in the *PITX1* expressing plasmid, using the Q5® Site-Directed Mutagenesis Kit (New England Biolabs).

To characterize *in vitro* missense variants of *PITX1*, we used COS7 cells since they do not have endogenous expression for this gene, and because they were previously used to study the first *PITX1* missense variant described in the literature (Gurnett et al., 2008). COS7 cells were grown in Dulbecco's modified Eagle's medium supplemented with 10% fetal bovine serum, 1% L-glutamine and 0.5% antibiotics. About 5×10^5 cells were seeded on 12-well plates and 1.5×10^6 cells on six-well plates 24 hr before transfection. Cells were transfected using Lipofectamine™ 2000 (Invitrogen) according to the manufacturer's instructions.

Western blot analysis was performed. After 24 hr of transfection with the pCMV6-XL5-*PITX1* plasmid, proteins were extracted with Radioimmunoprecipitation assay buffer (Sigma-Aldrich) complemented with cOmplete™ Protease Inhibitor Cocktail (Roche). Protein concentration was determined by the bicinchoninic acid method and equal amounts of protein (20 µg) were electrophoresed in NuPAGE™ 4–12% Bis-Tris Protein Gels (Invitrogen) then transferred to nitrocellulose membrane with iBlot™ two Gel Transfer Device (Invitrogen). Membranes were blocked with milk, and primary antibody incubations were performed at room temperature for 2 hr (*PITX1*, 1:3,000, Proteintech) or overnight at 4°C (Tubulin beta, 1:5,000, Elabscience). Secondary antibody horseradish peroxidase (HRP)-conjugated antirabbit (1:5,000, Santa Cruz Biotechnologies) and HRP-conjugated antimouse (1:4,000, SouthernBiotechnologie) were incubated for 1 hr at room temperature and detected with SuperSignal™ West Dura (Thermo Fisher Scientific). Protein bands were visualized with iBright™ CL1500 Imaging System (Thermo Fisher Scientific). Western blots were performed three times. Quantification was performed using the ImageJ software and statistical analysis using the Student's *t* test with Microsoft Excel software.

To perform immunofluorescence studies, transfected COS7 cells were fixed for 30 min in 4% paraformaldehyde, washed three times in phosphate-buffered saline (PBS) and permeabilized in PBS-0.2% Triton for 10 min. The fixed cells were blocked with PBS-4% bovine serum albumin-Tween 0.05% for 1 hr at room temperature and incubated with rabbit primary antibody at room temperature for 2 hr (*PITX1*, 1:200, Proteintech). After washing, the cells were incubated with secondary antibody at room temperature for 1 hr (Rabbit Alexa 555, 1:1,000, Thermo Fisher Scientific). After counterstaining with 4',6-diamidino-2-phenylindole, cells were visualized using confocal microscopy (Zeiss LSM170 Airyscan).

Reporter assays were also performed. After 48 hr of transfection with the pCMV6-XL5-PITX1 and TK-Bic-Luc plasmids, COS7 cells were washed twice with PBS and lysed with passive lysis 5× buffer (Promega). *Renilla* and Firefly luciferase reporter activities were assessed with the Dual-Luciferase Reporter Assay (Promega) according to the manufacturer's protocol, using the GloMax® Navigator Microplate Luminometer (Promega). Three transfection experiments were performed in triplicate. Statistical analysis was performed using the Student's *t* test with Microsoft Excel software.

Individual 1 was the first child of European nonconsanguineous parents. Intrauterine growth restriction (IUGR) and polyhydramnios were noted during the third trimester of pregnancy. Amniocentesis was performed and amniotic fluid standard G-band karyotype was normal. He was born at term by cesarean section. At birth, weight, length, and occipital-frontal circumference (OFC) were 2,440 g (≤ -2 standard deviation [SD]), 45.5 cm (-3 SD), and 34.3 cm (-0.5 SD), respectively. Microretrognathia with feeding difficulties and bilateral cryptorchidism were noted, as well as flexion deformity of knees requiring physical therapy and splinting. At the age of 3 years and 8 months, weight, height, and OFC were 12.400 kg (-2 SD), 89.5 cm (-2.5 SD), and 50 cm (-0.5 SD), respectively. Facial features included narrow palpebral fissures, low-set ears, micrognathia, and a thin nose. Limitation of knee extension, hyperlordosis, short toes, and equinus deformity of the feet were also noted; upper limbs were normal (Figure 1a–c). Skeletal survey, performed at the age of 3 years and 8 months, showed a small mandible with an obtused mandibular angle (Figure 1d), narrow iliac wings with an hourglass configuration, wide pubic symphysis (Figure 1e) and absence of patellar ossification (normal range of patellar ossification in boy: 2–6 years of age; Sarkodieh & Gobindpuri, 2016). At last examination at 7 years and 5 months of age, weight, height, and OFC were 19 kg (-2 SD), 112 cm (-2 SD), and 52.5 cm (M), respectively. Patellae were palpable but knee radiographs confirmed a marked patellar ossification delay (Figure 1f; Sarkodieh & Gobindpuri, 2016). He achieved normal neurodevelopment milestones: he sat unsupported at 7 months of age, and walked at 17 months of age on tiptoes due to the knee deformity. He has normal speech development; he attends mainstream school. He was referred to an endocrinologist for short stature and undescended testes. He underwent surgical interventions for cryptorchidism at the age of 15 months and 5 years. At 5 years and 7 months, bone age was evaluated at 3.5 years and hormonal tests ruled out growth hormone deficiency. Anti-Müllerian Hormone blood levels were low (300 pmol/L, normal range: 441–2,352), suggesting possible testicular dysfunction. Renal ultrasounds scan (USS) revealed left renal hypoplasia and renal function tests showed mild stable renal insufficiency (blood creatinine level: 57 μ mol/L, normal range: 30–48). Echocardiography was normal and 200 kb chromosomal microarray (CMA) ruled out cryptic chromosomal imbalances.

Individual 1's mother (Individual 2) showed a similar phenotype. She was the only child of healthy non-consanguineous parents. IUGR was noted during pregnancy. She was born at term; her birth weight was 2,200 g (-2.5 SD). She had micrognathia requiring orthodontic appliances. Short stature was noted and growth hormone therapy

was given from the age of 7–17 years. She had hyperlordosis requiring corset and knee instability due to patellar hypoplasia requiring left trochleoplasty. She gave birth to her child by cesarean section due to a narrowed pelvis. At the age of 33 years, her height was 160 cm (-0.5 SD; estimated mean parental height: -1 SD). Facial features included narrow palpebral fissures, a thin nose, and a small mandible. A skeletal survey confirmed narrow iliac wings and lumbar hyperlordosis (Figure 1g,h). Renal USS and creatinine and urea blood levels were normal.

Individual 3 is a boy born to healthy non-consanguineous European parents, unrelated to Individual 1 and 2. The couple had one termination of pregnancy for Down syndrome, and two miscarriages in the first trimester. Pregnancy, obtained by in vitro fertilization with intracytoplasmic sperm injection, was uneventful. He was born at 38 weeks of gestation by cesarean section for fetal distress. At birth, his weight, length and OFC were 3,130 g (0 SD), 49 cm (-0.5 SD), and 33 cm (-1.2 SD), respectively. Pierre–Robin sequence was noticed (Figure 1i) as well as micropenis, bilateral cryptorchidism, and severe knee flexion deformity. He underwent surgical interventions for cleft palate and knee deformity. At last examination at the age of 6 years, weight, length, and OFC were 16.8 kg (-1.5 SD), 113 cm (0 SD), and 51.2 cm (-0.5 SD), respectively. Facial features included narrow palpebral fissures, micrognathia, and a thin nose (Figure 1j). Psychomotor development is normal and he attends a mainstream school but he is still unable to walk unsupported and needs wheelchair, due to persistent severe knee flexion deformity.

Skeletal radiographs revealed mildly narrow iliac wings and a wide pubic symphysis (Figure 1l). Knee magnetic resonance imaging (MRI), performed at the age of 2 years and 10 months, confirmed patellar agenesis (Figure 1m). Heart and renal USS, CMA, and molecular analysis of the *TBX4* gene (Sanger sequencing and MLPA) were normal.

Exome sequencing (ES) performed in Individual 1 found a heterozygous missense variant in *PITX1* (NM_002653.4:c.793G>T, p.(Gly265Cys);Chr5(GRCh37):g.134364621C>A), which was confirmed by Sanger sequencing. Sanger molecular analysis confirmed the presence of the variant in Individual 2 and ruled it out in her parents (thus confirming its de novo occurrence in Individual 2).

ES performed in Individual 3, found a heterozygous missense variant in *PITX1* (NM_002653.4:c.412A>C, p.(Lys138Gln);Chr5(GRCh37):g.134365002T>G), which was confirmed by Sanger sequencing. Individual 3's phenotypically normal father carried the variant in a mosaic status (6% of leukocytes).

These two missense variants are predicted to be “disease causing” by the SIFT and Mutation taster software, and possibly damaging by Polyphen-2 (with a score of 1 and 0.997, respectively). They were absent from the gnomAD database of control individuals.

Parentage was confirmed by studying a subset of 30 common single nucleotide polymorphism positions in all samples of the run. Using the ACMG classification, the following criteria were present for both variants: PS2 (de novo), PM2 (absent from controls), PP3 (pathogenic bioinformatics prediction), and PP4 (monogenic etiology is the main hypothesis), leading to Class 4 variants (likely pathogenic).



FIGURE 1 Clinical and radiological features of Individuals 1–3. (a–f) Individual 1. At the age of 3 years and 8 months (a) and 6 years and 6 months (b and c), note narrow palpebral fissures, low-set ears, thin nose, small mandible, knee flexion deformity, hyperlordosis, and short toes. Radiographs, performed at the age of 3 years and 8 months, showed a small mandible with an obtused mandibular angle (d, arrow); narrow iliac wings with an hourglass configuration, and wide pubic symphysis (e). At the age of 7 years and 5 months, knee radiographs confirmed a marked delay in patellar ossification with a tiny ossification center (f, arrow; normal range of patellar ossification in boy: 2–6 years of age; Sarkodieh & Gobindpuri, 2016). (g and h) Individual 2. Radiographs showed narrow iliac wings and hyperlordosis (arrows). (i–m) Individual 3. Note, at the age of 10 days, posterior cleft palate associated with Pierre–Robin sequence (i); at the age of 3 years and 3 months, note narrow palpebral fissures, micrognathia, a thin nose, and persistent severe knee flexion deformity (j and k). Pelvis radiographs at birth, showing mildly narrow iliac wings, and wide pubic symphysis (l). Right knee MRI, sagittal T1-weighted sequence, at the age of 2 years and 10 months, showing patellar agenesis (arrow); the extensor apparatus is exclusively tendinous and dislocated laterally (m)

No other candidate variants were found in other genes with overlapping phenotype. Concerning ES performed in Individual 1, the coverage at 10× was 100% for *TBX4* and *SOX9*, and mean coverage was 98.5%. Concerning Individual 3, molecular analysis of *TBX4* was normal; the ES coverage at 10× was at 96.6% and 100% regarding the mean coverage and *SOX9* respectively.

The p.(Lys138Gln) *PITX1* variant was predicted in silico to have the same conformation as the wild-type protein but this variant is

localized in the DNA-binding domain, thus strongly suggesting that it could disrupt the interaction of the transcription factor with DNA (Figure 2a). No model was available for the p.(Gly265Cys), located in the PIT-1 interaction domain.

Concerning functional studies, western blot of COS7-transfected cells expressing wild-type (WT) *PITX1* or its variants p.(Lys138Gln) and p.(Gly265Cys) showed neither size change nor significant quantitative variation in *PITX1* expression for *PITX1* missense variants

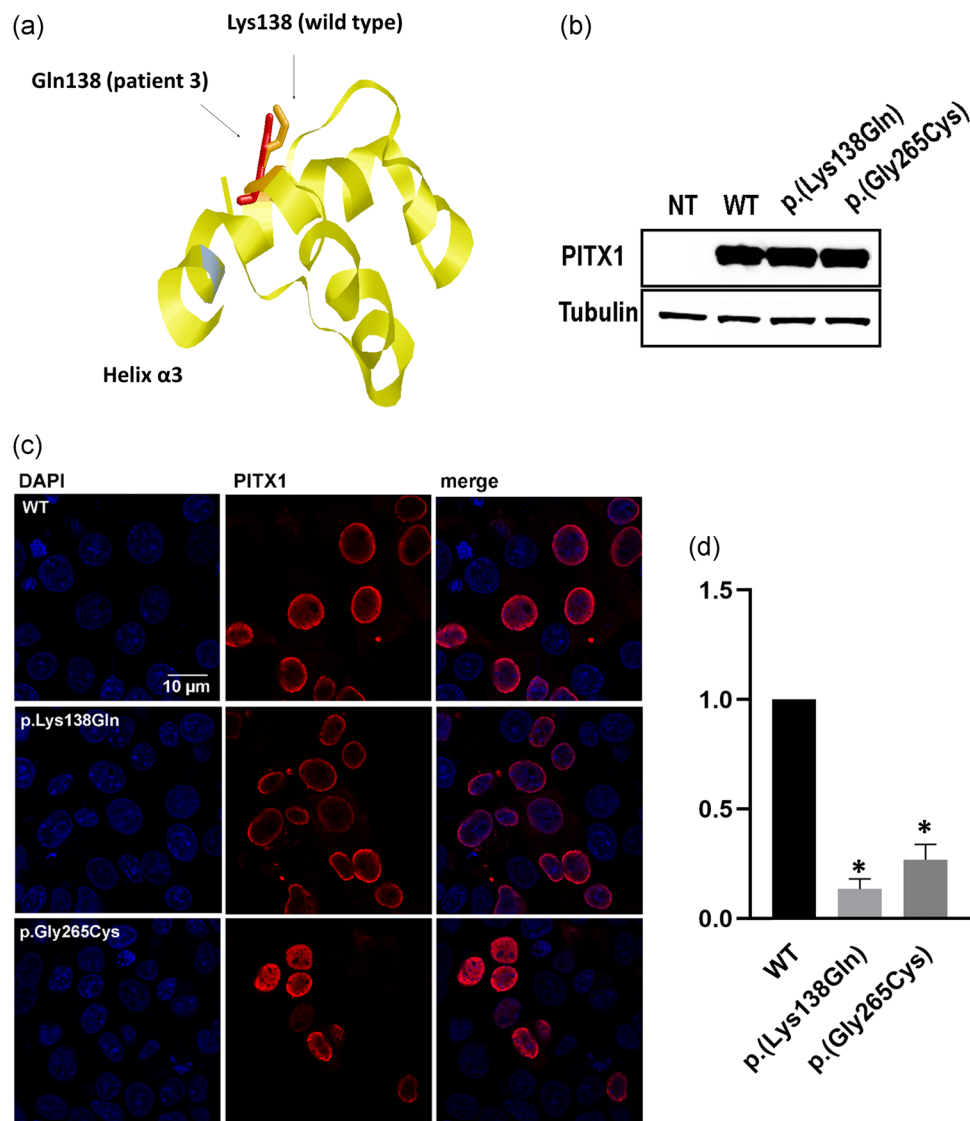


FIGURE 2 (a) 3D protein modeling of the human PITX1 homeodomain suggesting that the p.(Lys138Gln) variant does not affect protein conformation (confidence index: 99.8%–sequence identity: 93%) as compared with the native protein (confidence index: 99.8%–sequence identity: 95%). (b) Western blot of COS7-transfected cells expressing wild-type (WT) or mutated PITX1 p.(Lys138Gln) and p.(Gly265Cys). PITX1 is detected at 40 kDa and tubulin beta, a reference protein, is detected at 50 kDa. Neither size change nor significant quantitative variation in PITX1 expression is detected for missense variants compared with WT (*t* test). Hence, missense variants of PITX1 do not affect PITX1 expression. (c) Immunofluorescence staining of COS7-transfected cells expressing wild-type (WT) or mutated PITX1 p.(Lys138Gln) and p.(Gly265Cys). Visualization of the nuclei in blue by DAPI, of PITX1 in red and merge of the two staining. Missense variants of PITX1 do not affect PITX1 cellular localization. (d) Luciferase assays of COS7-transfected cells expressing wild-type (WT) and mutated PITX1 p.(Lys138Gln) and p.(Gly265Cys); ratio firefly/*Renilla* activity is normalized by the WT. These results show that missense variants of PITX1 significantly affect PITX1 transactivation (**p* < .05). NT, nontransfected cells; PITX1, paired-like homeodomain transcription factor 1

(Figure 2b). Immunofluorescence staining of COS7-transfected cells expressing WT or mutated PITX1, showed that missense variants of PITX1 do not affect PITX1 cellular localization, since the protein remains located into the nucleus (Figure 2c). To characterize the effects of the variants on transcription factor activity, we measured their ability to transactivate a reporter gene, as previously described (Gurnett et al., 2008). We cotransfected the PITX1 expression construct (pCMV6-XL5-PITX1) with a luciferase report construct (TK-Bic-Luc) consisting of a thymidine kinase promoter preceded by four

bicoid-binding sites. Luciferase assays of COS7-transfected cells expressing WT and mutated PITX1 showed that missense variants of PITX1 significantly affect PITX1 transactivation (Figure 2d). Compared with the WT, the transactivation ability is diminished 6.8 and 3.3-fold for p.(Lys138Gln) and p.(Gly265Cys) variants, respectively.

We report in this study a novel phenotypic spectrum of PITX1-RD characterized by mandibular hypoplasia possibly associated with Pierre-Robin sequence, narrowed iliac wings with an hourglass configuration, wide pubic symphysis, and patellar hypo/aplasia,

caused by novel *PITX1* missense variants. We propose to name this condition Mandibular-Pelvic-Patellar syndrome (MPP syndrome). Male urogenital abnormalities and prenatal onset short stature may be part of the phenotype as well, but further reports are needed to confirm this association.

PITX1 encodes a transcription factor mostly expressed in the lateral mesenchyme and the developing hindlimb bud, the pituitary gland and the derivatives of the first branchial arch. This gene plays an essential role in hindlimb morphogenesis by interacting with various transcription factors including *TBX4* and *SOX9* (Duboc & Logan, 2011; Wang, Infante, Park, & Menke, 2018).

PITX1 is part of a bicoid-related homeobox-gene family, including also *PITX2* (MIM# 601542) and *PITX3* (MIM# 602669). *PITX2* and *PITX3* are also involved in autosomal dominant human disorders: *PITX2* variants cause Axenfield-Rieger syndrome (MIM# 180500), anterior segment dysgenesis type 4 (MIM# 137600) or ring dermoid of cornea (MIM# 180550), and pathogenic variants in *PITX3* cause multiple subtypes of anterior segment dysgenesis (MIM# 107250) and cataract (MIM# 610623).

Two human *PITX1*-RD have been previously reported. Liebenberg syndrome, characterized by malformations of upper limbs acquiring radiological features similar to lower limbs, is caused by 5q31.1 rearrangements involving putative *PITX1* regulatory elements (Al-Qattan et al., 2013; Kragestein, Brancati, Digilio, Mundlos, & Spielmann, 2019; Mennen, Mundlos, & Spielmann, 2014; Seoighe et al., 2014, Spielmann et al., 2012). These structural genomic anomalies lead to the disruption of a topologically associated domain by deletion or removal of the *H2AFY* insulator. The alteration of the regulatory landscape results in an ectopic expression of *PITX1* in the forelimb buds, stimulated by the Pan-limb enhancer (*Pen*), which explains the development of a “lower limb morphology” (Kragestein et al., 2018).

Congenital clubfoot with or without deficiency of long bones and/or mirror-image polydactyly syndrome (CCF) was initially described by Gurnett et al. (2008). The reported propositus had bilateral clubfeet with preaxial polydactyly and right-sided tibial hemimelia. Among the eight affected relatives, five have clubfeet, and three have patellar hypoplasia. The p.(Glu130Lys) missense variant, located in the bicoid-related homeodomain, was identified in all the affected family members as well as in some phenotypically normal obligate carriers, suggesting incomplete penetrance. Functional analyses suggested the hypothesis of a dominant negative effect (Gurnett et al., 2008). Furthermore, Alvarado et al. (2011) described a 241 kb microdeletion identified in individuals from a three generations family presenting with isolated clubfoot. A *PITX1* intragenic deletion (c.765_799del, p.(Ala256Argfs*303)) was found in an individual with bilateral preaxial polydactyly, equinus talipes, and right-sided hemimelia (Klopocki et al., 2012). Two further fetuses described by Klopocki had talipes equinovarus and mirror-image polydactyly. Moreover, one of them had left single lower leg bone and the second one, a popliteal pterygium. These individuals carried deletions of respectively 4.9 and 5.7 Mb including *PITX1*. Finally, Rosenfeld et al. (2011) reported a few individuals carrying large deletions

including *PITX1* and clinically presenting with various multiple congenital abnormalities including, in one individual harboring a 8 Mb deletion, bilateral clubfeet, preaxial polydactyly, and Pierre-Robin sequence. Overall, CCF is caused by either *PITX1* haploinsufficiency or the missense p.(Glu130Lys) variant.

Szeto et al. (1999) reported a *Pitx1*^{-/-} mouse model showing a distinct phenotype including pelvis hypoplasia, patellar agenesis, mandibular hypoplasia, and cleft palate. Because *Pitx1* is expressed in the pituitary gland, these authors studied the mouse model pituitary cell types and demonstrated a reduction of gonadotrope and thyrotrope cells. Interestingly, 8.9% of *Pitx1*^{-/+} mice showed clubfoot-like features (Alvarado et al., 2011). The low penetrance of the limb malformations in the heterozygous mice compared with a high penetrance in humans has already been observed for other transcription factors involved in limb development, like *Lmx1b* (Chen et al., 1998). The phenotype of the three individuals reported in the present study shows striking similarities with the *Pitx1*^{-/-} mouse model, supporting that *PITX1* loss-of-function variants are responsible for MPP.

Functional analyses were previously designed by Gurnett et al. (2008) to characterize the missense variant p.(Glu130Lys) located in the DNA-binding domain and associated with CCF. We replicated these experiments to characterize the two missense variants associated with MPP phenotype: p.(Lys138Gln) located in the DNA-binding domain and p.(Gly265Cys) located in the PIT-1 interaction domain. Likewise the previously characterized variant, no significant quantitative or qualitative difference was observed on protein expression (Figure 2b) and mutant proteins remained located into the nucleus (Figure 2c). We showed, however, that both variants significantly affect *PITX1* transactivation ability on a reporter construct harboring several bicoid-binding sites (Figures 2d). The specific pathophysiological mechanism explaining the phenotypic differences between MPP syndrome and its allelic CCF syndrome currently remains unknown. Though no genotype-phenotype correlation can be made in such few cases, the location of the missense variant does not seem to explain the phenotypic differences. Indeed, both p.(Glu130Lys) and p.(Lys138Gln) are located in the bicoid-related homeodomain while associated with CCF and MPP, respectively. A dose-dependent gene transactivation defect may explain the variability of the phenotypic spectrum, since CCF-associated missense variant was responsible for a lower diminution of *PITX1* activity (around 1.7-fold, vs. 3.3–6.8-fold for MPP-associated missense variants). This hypothesis would be consistent with the low penetrance described in this CCF family (Gurnett et al., 2008), but it needs to be confirmed with the functional characterization of more missense variants associated with human diseases. In the *Pitx1* knockout mouse model, heterozygous mice show a low penetrance of clubfoot features reminding of the CCF phenotype, while homozygous mice show more severe skeletal features reminding of MPP (Szeto et al., 1999). This observation is consistent with the dose-dependent gene transactivation defect hypothesis too.

The main features of the *PITX1*-RD are summarized in Table S1. The clinical phenotypes of Liebenberg and CCF syndromes

emphasize the important role of *PITX1* in limb development. Our report supports the role of *PITX1* in the development of the mandible, pelvis and male urogenital system, thus fitting with the functional evidence previously reported in the *Pitx1*^{-/-} mouse model (Szeto et al., 1999).

PITX1 closely interacts with *TBX4* and *SOX9* (Duboc & Logan, 2011; Wang et al., 2018). It is interesting to emphasize that MPP shows a phenotypic overlap with Ischiocoxopodopatellar syndrome (ICPPS) with or without pulmonary arterial hypertension (MIM# 147891), which is caused by *TBX4* haploinsufficiency. Individuals affected by ICPPS present with patellar agenesis or hypoplasia, pelvic anomalies (notably ischiopubic arch hypoplasia), and feet abnormalities; the possible presence of micrognathia and cleft palate has also been occasionally reported (Bongers, Van Kampen, Van Bokhoven, & Knoers, 2005). MPP syndrome also displays a partial clinical overlap with the phenotypic spectrum caused by *SOX9* variants or chromosomal rearrangements involving *SOX9* regulatory elements (Mansour et al., 2002; Matsushita et al., 2013), such as Pierre-Robin sequence, small pelvis, possible patellar hypoplasia, clubfoot, and male urogenital abnormalities.

In conclusion, we report two novel *PITX1* missense variants, altering *PITX1* transactivation ability, in three individuals from two unrelated families showing a distinct recognizable syndrome including first branchial arch, patellar, pelvic and male urogenital abnormalities. We propose to name this condition MPP syndrome. Our study findings expand the spectrum of *PITX1*-RD and suggest a common pattern of developmental abnormalities in disorders of the *PITX1*-*TBX4*-*SOX9* signaling pathway.

ACKNOWLEDGMENTS

The authors would like to thank individuals and their family for their collaboration; Biolmaging Center, Lille, France, for confocal microscopy; Dr. Christina A. Gurnett, Washington University, USA, for providing plasmids; Sylvie Mazoyer, GENDEV Team, Bron, France, for critical reading of the manuscript.

CONFLICT OF INTERESTS

The authors declare that there are no conflicts of interests.

AUTHOR CONTRIBUTIONS

G. M. collected the clinical, molecular and functional data, and wrote the paper with M. R. C. D., S. B., F. F., and F. P. performed and interpreted functional tests. G. L., N. C., A. L., D. S., J. T., L. F., and F. E. interpreted molecular analyses. A. F., O. P., and D. G. provided clinical and radiological data. P. E. and S. M. gave expert clinical opinion. D. G. and M. R. coordinated the study. All authors approved the final version of the manuscript.

DATA AVAILABILITY STATEMENT

The data that support the findings of this study are available from the corresponding author upon reasonable request. The novel *PITX1* variant information was submitted to the ClinVar database (<https://www.ncbi.nlm.nih.gov/clinvar/>) (SUB7608370; SUB7643212).

ORCID

Nicolas Chatron  <http://orcid.org/0000-0003-0538-0981>

Florence Petit  <http://orcid.org/0000-0002-1368-1023>

Massimiliano Rossi  <http://orcid.org/0000-0002-5797-8152>

REFERENCES

- Al-Qattan, M. M., Al-Thunayan, A., Alabdulkareem, I., & Al Balwi, M. (2013). Liebenberg syndrome is caused by a deletion upstream to the *PITX1* gene resulting in transformation of the upper limbs to reflect lower limb characteristics. *Gene*, 524(1), 65–71. <https://doi.org/10.1016/j.gene.2013.03.120>
- Alvarado, D. M., McCall, K., Aferol, H., Silva, M. J., Garbow, J. R., Spees, W. M., ... Gurnett, C. A. (2011). *Pitx1* haploinsufficiency causes clubfoot in humans and a clubfoot-like phenotype in mice. *Human Molecular Genetics*, 20(20), 3943–3952. <https://doi.org/10.1093/hmg/ddr313>
- Bongers, E., Van Kampen, A., Van Bokhoven, H., & Knoers, N. (2005). Human syndromes with congenital patellar anomalies and the underlying gene defects. *Clinical Genetics*, 68(4), 302–319. <https://doi.org/10.1111/j.1399-0004.2005.00508.x>
- Chen, H., Lun, Y., Ovchinnikov, D., Kokubo, H., Oberg, K. C., Pepicelli, C. V., ... Johnson, R. L. (1998). Limb and kidney defects in *Lmx1b* mutant mice suggest an involvement of *LMX1B* in human nail patella syndrome. *Nature Genetics*, 19(1), 51–55. <https://doi.org/10.1038/ng0598-51>
- Duboc, V., & Logan, M. P. O. (2011). *Pitx1* is necessary for normal initiation of hindlimb outgrowth through regulation of *Tbx4* expression and shapes hindlimb morphologies via targeted growth control. *Development*, 138(24), 5301–5309. <https://doi.org/10.1242/dev.074153>
- Gurnett, C. A., Alaee, F., Kruse, L. M., Desruisseau, D. M., Hecht, J. T., Wise, C. A., ... Dobbs, M. B. (2008). Asymmetric lower-limb malformations in individuals with homeobox *PITX1* gene mutation. *The American Journal of Human Genetics*, 83(5), 616–622. <https://doi.org/10.1016/j.ajhg.2008.10.004>
- Klopocki, E., Kähler, C., Foulds, N., Shah, H., Joseph, B., Vogel, H., ... Kurth, I. (2012). Deletions in *PITX1* cause a spectrum of lower-limb malformations including mirror-image polydactyly. *European Journal of Human Genetics*, 20(6), 705–708. <https://doi.org/10.1038/ejhg.2011.264>
- Kragestein, B. K., Brancati, F., Digilio, M. C., Mundlos, S., & Spielmann, M. (2019). H2AFY promoter deletion causes *PITX1* endoactivation and Liebenberg syndrome. *Journal of Medical Genetics*, 56(4), 246–251. <https://doi.org/10.1136/jmedgenet-2018-105793>
- Kragestein, B. K., Spielmann, M., Paliou, C., Heinrich, V., Schöpflin, R., Esposito, A., ... Andrey, G. (2018). Dynamic 3D chromatin architecture contributes to enhancer specificity and limb morphogenesis. *Nature Genetics*, 50(10), 1463–1473. <https://doi.org/10.1038/s41588-018-0221-x>
- Liebenberg, F. (1973). A pedigree with unusual anomalies of the elbows, wrists and hands in five generations. *South African Medical Journal*, 47(17), 745–748.
- Maiti, R., Van Domselaar, G. H., Zhang, H., & Wishart, D. S. (2004). SuperPose: A simple server for sophisticated structural superposition. *Nucleic Acids Research*, 1(32), W590–4. <https://doi.org/10.1093/nar/gkh477>
- Mansour, S., Offiah, A., McDowall, S., Sim, P., Tolmie, J., & Hall, C. (2002). The phenotype of survivors of campomelic dysplasia. *Journal of Medical Genetics*, 39(8), 597–602. <https://doi.org/10.1136/jmg.39.8.597>
- Matsushita, M., Kitoh, H., Kaneko, H., Mishima, K., Kadono, I., Ishiguro, N., & Nishimura, G. (2013). A novel *SOX9* H169Q mutation in a family with overlapping phenotype of mild campomelic dysplasia and small patella syndrome. *American Journal of Medical Genetics, Part A*, 161A(10), 2528–2534. <https://doi.org/10.1002/ajmg.a.36134>
- Mennen, U., Mundlos, S., & Spielmann, M. (2014). The Liebenberg syndrome: In depth analysis of the original family. *The Journal of*

- Hand Surgery (European Volume)*, 39(9), 919–925. <https://doi.org/10.1177/1753193413502162>
- Rosenfeld, J. A., Drautz, J. M., Clericuzio, C. L., Cushing, T., Raskin, S., Martin, J., ... Shaffer, L. G. (2011). Deletions and duplications of developmental pathway genes in 5q31 contribute to abnormal phenotypes. *American Journal of Medical Genetics, Part A*, 155(8), 1906–1916. <https://doi.org/10.1002/ajmg.a.34100>
- Sarkodieh, J., & Gobindpuri, A. (2016). *The age of patella ossification*. Poster presented at the meeting European Society of Musculoskeletal Radiology, Zurich, Switzerland.
- Seoighe, D. M., Gadancheva, V., Regan, R., McDaid, J., Brenner, C., Ennis, S., ... Lynch, S. A. (2014). A chromosomal 5q31.1 gain involving *PITX1* causes Liebenberg syndrome. *American Journal of Medical Genetics, Part A*, 164(11), 2958–2960. <https://doi.org/10.1002/ajmg.a.36712>
- Spielmann, M., Brancati, F., Krawitz, P. M., Robinson, P. N., Ibrahim, D. M., Franke, M., ... Mundlos, S. (2012). Homeotic arm-to-leg transformation associated with genomic rearrangements at the *PITX1* locus. *American Journal of Human Genetics*, 91(4), 629–635. <https://doi.org/10.1016/j.ajhg.2012.08.014>
- Szeto, D. P., Rodriguez-Esteban, C., Ryan, A. K., O'Connell, S. M., Liu, F., Kioussi, C., ... Rosenfeld, M. G. (1999). Role of the Bicoid-related homeodomain factor Pitx1 in specifying hindlimb morphogenesis and pituitary development. *Genes & Development*, 13(4), 484–494.
- Wang, J. S., Infante, C. R., Park, S., & Menke, D. B. (2018). *PITX1* promotes chondrogenesis and myogenesis in mouse hindlimbs through conserved regulatory targets. *Developmental Biology*, 434(1), 186–195. <https://doi.org/10.1016/j.ydbio.2017.12.013>

SUPPORTING INFORMATION

Additional supporting information may be found online in the Supporting Information section.

How to cite this article: Morel G, Duhamel C, Boussion S, et al. Mandibular-pelvic-patellar syndrome is a novel *PITX1*-related disorder due to alteration of *PITX1* transactivation ability. *Human Mutation*. 2020;41:1499–1506. <https://doi.org/10.1002/humu.24070>